Wavelength Bistability and Switching in Two-Section Quantum-Dot Diode Lasers

Mingming Feng, Steven T. Cundiff, Richard P. Mirin, *Senior Member, IEEE*, and Kevin L. Silverman

Abstract—We report lasing wavelength bistability with respect to applied bias on the saturable absorbers in two-section mode-locked quantum dot lasers. We show data from three different devices exhibiting wavelength bistability. All lasers display wavelength bistability. Only one lasing wavelength is present at a time, with all other wavelengths totally quenched. The switchable ranges (the wavelength difference between two bistable lasing branches) are different for all three lasers and in one device can be manipulated by changing the current injection. All lasers show the remarkable property of switching only in integer multiples of about 8 nm. The bistable operation can be explained by the interplay of the cross-saturation and self-saturation properties in gain and absorber, and the quantum-confined Stark effect in absorber. The measured switching time between bistable wavelengths is 150 ps.

Index Terms—Diode laser, mode-locked, quantum dot, wavelength bistability.

I. INTRODUCTION

WAVELENGTH bistable lasers are attractive devices for incorporation in next-generation optical networks where the time consuming and component-intensive tasks of optical-to-electrical and electrical-to-optical conversion need to be minimized [1]. They may be employed as compact and fast wavelength switching devices or as memory elements in photonic circuits, due to their robust latching properties [2], [3]. For such devices to be cost competitive they should also be compatible with chip-level optical architecture. Therefore, monolithic devices such as semiconductor diode lasers are more desirable than other types of optical bistable lasers, such as fiber lasers and external cavity lasers [4]. Conventional diode lasers do not normally exhibit wavelength bistability, so we must look to a design with added flexibility but still monolithic. Two-section diode lasers that are currently being used to generate ultrafast mode-locked pulses are a potential

candidate. Working with mode-locked lasers also offers the additional advantage of being able to support extremely high speed applications.

In two-section diode lasers, the ability to separately control the gain and absorbing regions can lead to various forms of optical bistability. In particular, these lasers can exhibit power bistability when the current applied to the gain section is swept [5]–[7]. Wavelength bistability has been more difficult to achieve but has been observed in continuous-wave, two-section distributed feedback (DFB) diode lasers almost two decades ago [8]. There have been relatively few results on bistable wavelength diode lasers since then [1]. In the last few years, the success of mode-locked two-section quantum dot (QD) diode lasers has led to new and exciting results in the area of wavelength bistability [9]. For example, bistability was recently demonstrated between the ground and excited state transitions of the QD gain medium [10]. In this case the subordinate mode was not completely quenched throughout the bistable region, possibly due to the fact that cross-gain saturation between ground and excited states was not strong enough. In our earlier work, we reported wavelength bistability from a two-section QD diode laser with a very high contrast between two lasing wavelengths both supported by the ground state gain [9]. To further investigate this phenomenon we have fabricated and tested additional devices with slightly different structures and measured the dynamics of the switching process. The new structures also exhibit markedly different switching characteristics from which we can glean important new information.

In this paper, we present our investigation of wavelength bistability in two-section QD diode lasers. We first discuss analyze simplified coupled mode equations as a model for the observed bistability. With this simple understanding we can explain why the unique gain dynamics of quantum dot ensembles lead to some of the new results. We then present our experimental results on wavelength bistability from three different two-section passively mode-locked diode lasers. The devices are not always mode-locked, but we restrict our investigation to devices working in the stable mode-locked region. All three lasers show wavelength bistability when the reverse bias voltage on the saturable absorber is swept, but have different wavelength spacings between two bistable branches. Because our lasers operate in the mode-locked region, there are a group of longitudinal modes in one lasing wavelength. In this paper, the word 'mode' refers to one lasing wavelength.

M. Feng is with JILA, National Institute of Standards and Technology and University of Colorado, Boulder, CO 80309-0440 USA and Department of Physics, University of Colorado, Boulder, CO 80309-0390 USA (e-mail: mingming.feng@colorado.edu).

S. T. Cundiff is with JILA, National Institute of Standards and Technology and University of Colorado, Boulder, CO 80309-0440 USA (e-mail: cundiffs@jila.colorado.edu).

R. P. Mirin and K. L. Silverman are with the National Institute of Standards and Technology, Boulder, CO 80305 USA (e-mail: mirin@boulder.nist.gov; silverma@boulder.nist.gov).

II. MODE COMPETITION IN TWO-SECTION LASERS

To gain a general understanding of the important features of our bistable laser we analyze a simplified set of coupled differential equations [11]. The two-section laser contains regions

of both saturable gain and absorption in which lasing modes experience gain or loss and interact with each other. If we include both gain and absorption regions in the same term, assume fast dynamics in the gain and saturable absorber and make a "weak" saturation approximation, then the intensities of two lasing modes, I_1 and I_2, evolve according to rate equations

$$\frac{dI_1}{dt} = (\alpha_1 - \beta_1 I_1 - \theta_{12} I_2) \times I_1, \tag{1a}$$

$$\frac{dI_2}{dt} = (\alpha_2 - \beta_2 I_2 - \theta_{21} I_1) \times I_2, \tag{1b}$$

where α_i is the small-signal gain minus loss for each mode, and β_i and θ_{ij} represent the self- and cross-saturation coefficients. These are the Lotka-Volterra equations, which are often used to describe competition between biological species [12]. For certain values of the constants in (1), there are exactly two steady state solutions that are characterized by nonzero intensity in only one of the two potential modes. These solutions corresponds to one mode (species) always winning out over the other regardless of initial conditions. We are interested in the case in which both modes are simultaneously stable. If this solution is stable to small perturbations then both modes will coexist in the steady state. If this point in not stable, the system will progress towards one or the other solutions with its ultimate destination being determined by initial conditions. Bistability occurs in this regime.

To reveal the conditions required for bistable operation we can perform a perturbation analysis around the dual mode solution. This point is unstable, and therefore bistable behavior is predicted if

$$\frac{\theta_{12}\theta_{21}}{\beta_1 \beta_2} > 1. \tag{2}$$

This condition requires the cross-saturation between the two modes to be stronger than the self-saturation. Obviously achieving this condition is quite difficult in a single section laser. On the other hand, if we include a separate saturable absorption region, the cross-saturation term now consists of two terms

$$\theta_{12} \approx \theta_{21} = \theta_{12}^g - \theta_{12}^a, \tag{3}$$

as does the self-saturation term

$$\beta_1 \approx \beta_2 = \beta_1^g - \beta_1^a. \tag{4}$$

These add flexibility such that (2) can be satisfied in a system with strong cross-saturation in the gain region and weak cross-saturation in the absorption region. One final consideration is that the overall gain in the two potential modes must be similar. Without this balance, the dual mode solution will no longer satisfy (2), and stable single-mode operation will prevail.

It is possible to extend the analysis presented here by including full saturation of the absorption and gain [13]. This model predicts more exotic forms of bistability such as that observed in [10] where single mode and dual mode operation are bistable with respect to each other.

III. QUANTUM DOT ACTIVE REGIONS

All of the two-section mode-locked lasers detailed in this paper feature self-assembled semiconductor quantum dots as the gain medium. Electrons and holes are strongly confined in three dimensions, and therefore QDs exhibit unique optical and electrical characteristics [14]–[16]. This confinement results in a strong dependence of transition energy on the size and shape of the QDs, leading to a large inhomogeneous broadening and making them promising in broad bandwidth applications such as ultrafast lasers. Ideally, the individual QDs will have a narrow Lorentzian lineshape similar to an atom. In reality, these optical transitions are broadened dramatically with increased temperature due to exciton-phonon coupling and with increased carrier injection due to carrier-carrier scattering [14]. It is these properties that ensure the optical properties of the QDs in the gain and absorption regime are quite different from one another.

The gain region is subjected to extremely high carrier injection levels. There are high carrier densities not just in the QDs, but also in the barrier regions where electrons and holes are free to move throughout the device. This leads to strong coupling between QDs at different energies since they all must compete for the same carriers in the barrier region. In addition to this effect, carrier-carrier scattering dominates at these densities and leads to strong dephasing of the individual QD transitions, resulting in very large homogeneous broadening. These two mechanisms both contribute to the strong cross-saturation between energetically separated photon modes being simultaneously amplified in QD active media [14]–[16].

The situation is quite different in the absorbing region of the device. Here, a reverse bias is applied, and the entire region is depleted of carriers. Therefore the carrier-carrier scattering that broadened the transition in the gain region is almost completely absent. Instead the width of the transition is limited by the slower carrier-phonon scattering rate. The result is a much narrower homogeneous line of approximately 8 nm [14]. Coupling through the carrier reservoir is also greatly reduced as compared to the gain region. This reduction occurs because electrons and holes generated in the QDs by absorption of photons are swept out of the active region by the applied electric field and are not allowed to reenter the other QDs. The self-saturation coefficients also differ between the gain and absorption sections. This is because of the faster recovery dynamics in the gain section which leads to a slightly higher saturation value.

It is the unique saturation properties discussed above that make QDs a promising candidate for satisfying (2). The extremely broad inhomogeneous spectrum ensures that even widely spaced modes have similar gain. The two qualities together make QDs an ideal system in which to investigate wavelength bistability.

IV. EXPERIMENTS AND RESULTS

We fabricated and tested three different two-section QD lasers. A schematic of a generic laser design is shown in Fig. 1, as in [9]. It consists of a two-section ridge waveguide where one section is electrically pumped while the other section is reverse biased as a saturable absorber. The active region of all devices consists of a tenfold stack of InGaAs QDs layers embedded in a
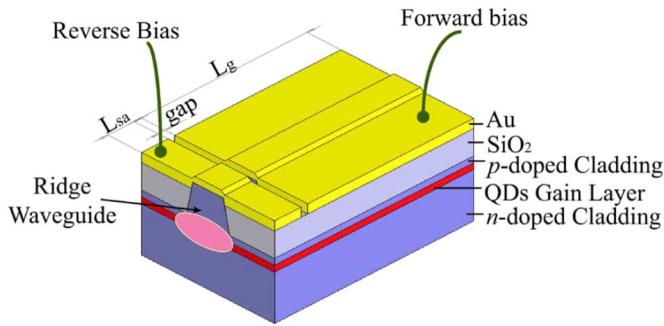
Fig. 1. Schematic of a two-section QD diode laser [9].
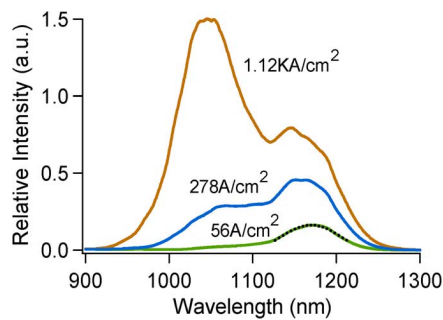
Fig. 2. Electroluminescence spectra of QD gain.

GaAs waveguide, which is sandwiched between $Al_{0.7}Ga_{0.3}As$ cladding layers. The waveguide was fabricated by standard photolithography and wet etching. A strip waveguide was etched in the top cladding layer followed by the removal of a small section of the heavily doped cap layer to provide isolation between the two sections. The lengths of the gain section and the saturable absorber section are L_g and L_{sa}, respectively. P-and n-type ohmic contacts were established with Ti/Au and Ni/AuGe/Ni/Au, respectively. No coating was applied to the cleaved facets. The device was mounted p-side up on a copper heat sink that was thermoelectrically temperature controlled.

The same QD material was used in all three devices. The QDs have a ground state (GS) transition at $\sim$1170 nm, with a full-width at half maximum of 60 nm, as determined by a fit to the low excitation electroluminescence data in Fig. 2. At higher injection levels, an excited state (ES) centered at approximately 1050 nm becomes apparent. This broad, inhomogeneous, gain spectrum is indicative of the size/shape distribution of the QD ensemble.

It is interesting that the gain spectrum becomes fairly flat over an approximately 200 nm range at injection levels around 300 A/cm^2. This situation leads to interesting mode competition effects in the laser cavity as discussed above.

Wavelength bistability is studied in three different laser geometries. The relevant parameters for the three different lasers are summarized in Table I. All three lasers exhibit similar characteristics, thus we will discuss the general features of the first device in depth as a representative example and then compare and contrast all three devices.

TABLE I
RELEVANT PARAMETERS COMPARISON FOR THE THREE DEVICES

	Lg (mm)	Lsa (mm)	Waveguide width (μm)	Threshold Current density Jth (A/cm2)
Device One	5.5	0.3	6	136
Device Two	5.5	0.3	6	142
Device Three	2.8	0.3	8	290

A. Device One

The first device we tested has a waveguide width of 6 μm. The length of the gain section (L_g) is 5.5 mm, and the length of the saturable absorber section (L_{sa}) is 0.3 mm. The operating temperature is 12°C. With the saturable absorber region electrically floating, the threshold current is 45 mA (threshold current density is 136 A/cm^2), and the lasing wavelength is 1173 nm.

The optical spectrum and output power of the QD laser were measured with current injection into the gain section and a reverse-bias voltage applied to the saturable absorber section. With a fixed reverse bias on the saturable absorber, the laser exhibits a hysteresis loop in the power-current characteristics [5], [6]. This typical behavior for mode-locked diode lasers can be attributed to the strong hole-burning in the absorber region that allows the laser to stay above threshold even when the injection level is brought below the unsaturated zero-gain point.

When the laser is operated with fixed injection current to the gain region and a varying bias on the saturable absorber region, hysteresis and bistability are observed in the lasing wavelength, as shown in Fig. 3(a). Throughout the saturable absorber bias range of -6 to -1 V, the laser has two stable wavelengths, 1163 nm and 1173 nm.

By comparing with the electroluminescence data in Fig. 2, it is clear that ground-state emission is responsible for both lasing states. As evident from Fig. 3(b), the two lasing modes are well separated, and the power contrast between them is more than 30 dB. The switchable wavelength range remains relatively constant throughout the region and is around 7.7 nm when $V_{sa} = -3$ V. Moreover, the power in each of the two lasing modes is almost identical, as shown in Fig. 3(c). For example, at $V_{sa} = -4$ V, the power ratio between 1173 nm (0.57 mW) and 1166 nm (0.62 mW) is 0.92.

We also found that wavelength bistability can be observed only in the narrow range of gain currents between 50 and 52 mA, as shown in Fig. 3(d). When the current is too low, the laser is either unstable or only one lasing wavelength is observed at a single saturable absorber bias voltage. When the current is too high, e.g., at the 55 mA shown in Fig. 3(d), the lasing wavelength varies almost continuously as the saturable absorber bias voltage is varied, and there is no bistability. Note that the bistable area at 52 mA is slightly bigger than the area at 50 mA, with the higher energy mode surviving at larger reverse biases. This is easily explained by the additional gain provided to the shorter wavelength mode at higher injection levels due to the strong state-filling effects in QDs. Therefore, the points where the gain of the two modes becomes dissimilar to support bistable operation moves to lower reverse bias voltage.
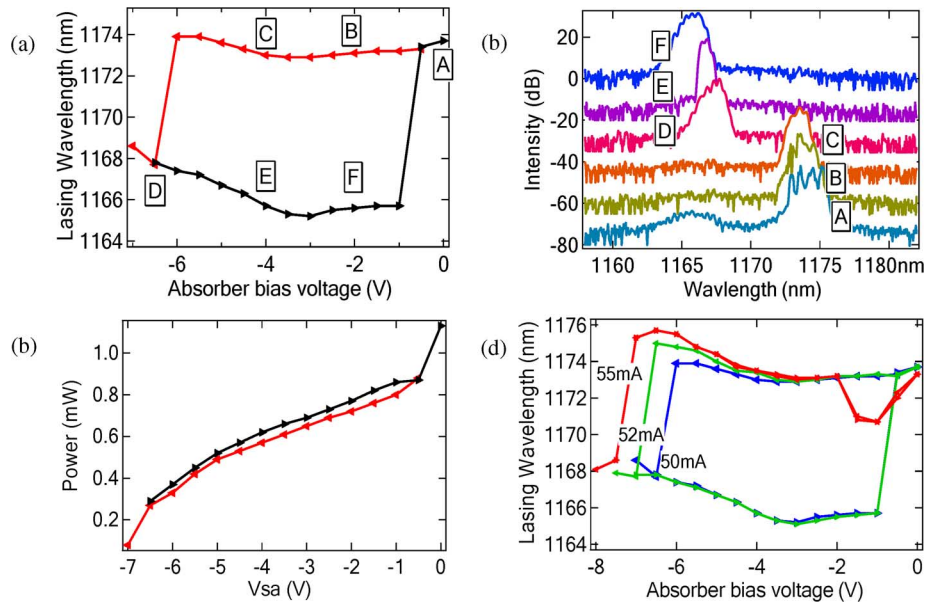
Fig. 3.   (a) Wavelength of laser emission as a function of saturable absorber bias (Vsa) at a fixed gain section current of 50 mA. (b) Optical spectra at various positions in the left hysteresis curve (the curves are offset for clarity). (c) Optical power as a function of Vsa. (d) Lasing wavelength vs Vsa at different gain currents. The left-pointing triangle "◁" means the trace is taken with the bias ramped up, from 0 to −7 V; The right-pointing triangle "▷" means the trace is taken with the bias ramped down, from −7 to 0 V.
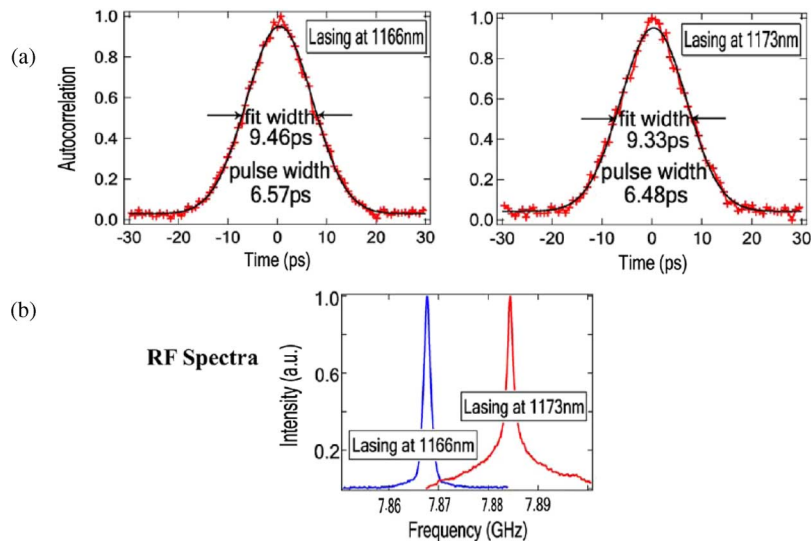
Fig. 4.   (a) Intensity autocorrelation for the mode-locked pulses on different branches of the hysteresis curve, both at −4 V reverse bias. (b) Corresponding radio-frequency spectra [9].

We also measured the pulse characteristics of the laser output in the two branches of the hysteresis loop shown in Fig. 3. We observed that stable mode-locking occurs in both branches of the hysteresis loop. An autocorrelation trace measured with the laser operating in each branch at $V_{sa} = -4$ V is displayed in Fig. 4(a). The corresponding pulse width is about 6.5 ps, assuming a Gaussian pulse shape, and is essentially identical in both branches. The pulse could be shortened by increasing the reverse bias, and the shortest value obtained is 3 ps at −6 V. Fig. 4(b) shows the radio-frequency (RF) spectra of the device. It indicates a pulse train with a repetition rate of around 7.9 GHz corresponding to a round trip time of 120 ps. The difference in frequency between the two branches is approximately 15 MHz,

with the longer wavelength branch at higher frequency, as expected from the normal dispersion in the GaAs waveguide.

B. Devices 2 and 3

We tested two other lasers exhibiting bistability (see Table I), a laser that was nominally identical to the first one but with a higher threshold current (device 2) and one with a different ratio of gain length to absorber length (device 3). As expected, device 2 showed qualitatively similar performance to device one. Bistability is observed at current injection levels between 55 mA and 64 mA, which is a slightly higher injection level than for device 1. Fig. 5(a) compares the two hysteresis curves. Device 2 exhibits a much larger wavelength spacing between the modes,
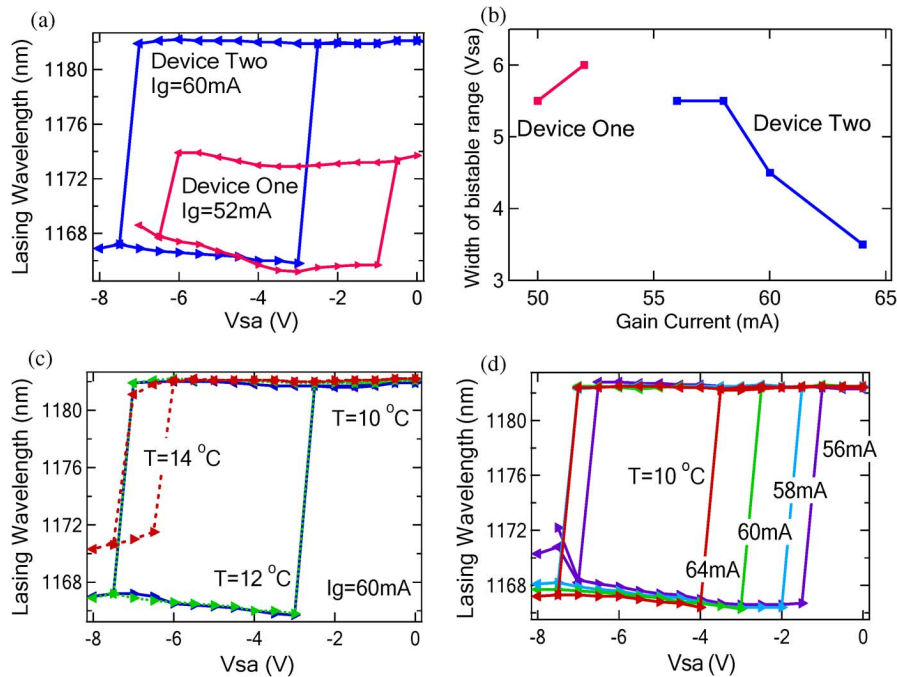
Fig. 5. Wavelength bistability comparison between device one (in red line) and device two (in blue line). (a) Laser emission as a function of saturable absorber bias (V_{sa}). (b) Vsa width of bistability at different gain current injection. Device two's lasing wavelengths as a function of saturable absorber bias (V_{sa}). Wavelength bistability data for Device two: (c) At different temperatures (gain current 60 mA). (d) At different gain currents. The left-pointing triangle "◁" means the trace is taken with the bias ramped up from 0 to −8 V. The right-pointing triangle "▷" means the trace is taken with the bias ramped down from −8 to 0 V.

with the shorter wavelength mode at approximately the same location. This result is consistent with the higher injection level producing a wider gain bandwidth due to stronger state-filling effects at higher current. These results clearly demonstrate the ability to tune the switchable range in this laser by simple adjustments to the amount of gain and/or loss present in the device.

In Fig. 5(b), we compare the width of the bistability region for the first two devices as a function of current injected to the gain section. The bistable region decreases with injection current for device two, which is the complete opposite behavior of the first device. The reason for this difference is that the hysteresis loop for device 2 collapses on the low energy side while device one shuts down on the higher energy side. Again this is consistent with the higher energy mode beginning to dominate at higher injection levels. The detail bistable data for device two are present in Fig. 5(c) for different device temperature and Fig. 5(d) for different gain current.

The third laser we tested had a different geometry, with $L_{sa} = 0.3$ mm, $L_g = 2.8$ mm, and a waveguide width $= 8$ μm. With the saturable absorber region floating and a temperature of 10°C, the threshold current is 65 mA (threshold current density is 290 A/cm^2). This threshold current density is about twice that of the first device because more injection current is needed to overcome the mirror loss due to a shorter gain segment. The initial lasing mode is at 1170 nm, which is slightly shorter than those of the first two devices. The reason is that the gain region current density is much higher for the third device, and the overall gain peak blue shifts because of state filling. With the significantly higher current density injection, the overall gain profile is much larger and flatter compared to the first two devices (see the EL spectra in Fig. 2) resulting in a very large

wavelength range in which modes experience similar amounts of gain. This fact leads to more complicated and interesting properties for device 3.

The wavelength-bias voltage hysteresis curve for the third device taken at various injection currents is shown in Fig. 6(a). The switchable range is 32 nm when the gain current is 88 mA (current density is 393 A/cm^2). When the current is increased to 96 mA (current density is 428 A/cm^2) and 100 mA (current density is 446 A/cm^2), the ranges change to 25 nm and 16 nm, respectively. The gain region current range for wavelength bistability is from approximately 84 mA to 104 mA. Throughout this region, the spacing between laser modes takes on three discrete values, as shown in Fig. 6(a).

We also show the power-bias voltage hysteresis curve in Fig. 6(b) for different pump currents. The power difference between the two branches is the biggest at low current. The difference decreases monotonically as the current is increased while the wavelength difference in the two branches decreases. To demonstrate the high isolation between the two lasing branches, a 3D optical spectrum is plotted for $I_g = 96$ mA in Fig. 6(c). The black arrow shows the direction of the sweep for the saturable absorber bias. The modes in the two branches are well distinguished and isolated.

The most interesting property of this device is that the switchable range changes with gain current, which did not happen with the first two devices. As the injection to the gain region is increased, the separation between the lasing modes becomes smaller. The longer wavelength mode stays relatively constant, while the shorter wavelength mode moves progressively longer. This behavior is different than the trend observed in the first two devices. It is also counterintuitive, since one would expect
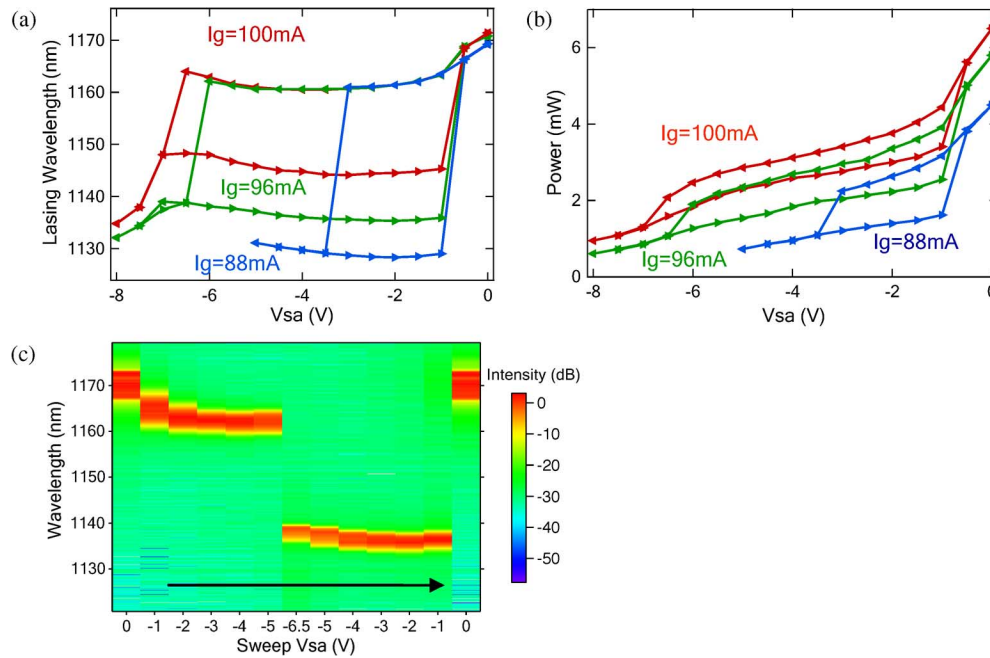
Fig. 6. Device 3 lasing wavelengths as a function of saturable absorber bias (V_{sa}). (a) Different gain currents when the temperature is $10°$C. (b) Power bistability at different currents. (c) 3D optical spectrum when V_{sa} is swept from 0 to -6.5 V and back to 0 V at $I_g = 96$ mA. The direction is shown by the arrow (the intensity is on a log scale). In (a) and (b), the left-pointing triangle "◁" means the trace is taken with the bias ramped up from 0 to -8 V; The right-pointing triangle "▷" means the trace is taken with the bias ramped down from -8 to 0 V.

higher energy modes to have relatively more gain at higher current densities, due to state filling.

There are two factors that, in combination, may be responsible for these results. At these higher current densities the gain curve is fairly flat, and therefore subtle changes can dictate which mode becomes the eventual winner. Because the gain curve is flat, the relative amounts of gain and loss determine where the gain peak occurs. Since the loss in the absorber region is monotonically increasing in this region (unlike the gain), the net gain peak shifts to lower energies as the relative strength of the absorption grows. This scenario fits well with the observation of higher energy modes lasing as the gain is increased (absorption relatively decreased).

C. Switching Mechanism

An additional requirement for a practical bistable laser is an effective switching mechanism. The lasers in this work can be switched electrically by modulating the bias voltage on the absorber. There is a strong red shift of the QD transition energy with the application of an electric field. This shift is known as the quantum-confined Stark effect (QCSE) and has been measured to be up to 2 nm/V in similar structures [17], [18]. The effect on the overall laser cavity (i.e., saturable absorber plus gain region) is to shift the peak gain to shorter wavelengths. Once one laser mode becomes too highly favored over the other, bistability breaks down and single mode operation occurs, causing the laser to abruptly change modes.

To measure this shift, we monitored the electroluminescence spectrum as a function of saturable absorber bias from the first laser. In this experiment, one of the facets was antireflection coated to inhibit lasing, and light was extracted from the facet adjacent to the saturable absorber region. The result is shown in
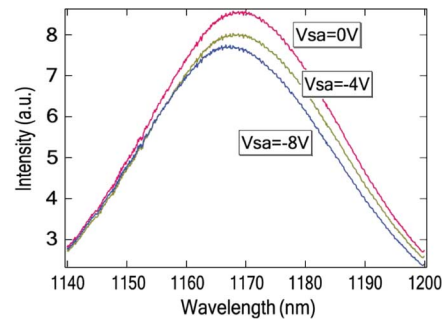
Fig. 7. Electroluminescence spectra taken from a sample similar to the first laser, but with an antireflection coating to inhibit lasing. The light was extracted from the facet adjacent to the saturable absorber region. V_{sa} is the bias voltage of the saturable absorber region [9].

Fig. 7. Although not a quantitative measure of the gain spectrum in our laser cavity, it is clear that the effect of the increased bias is not only to reduce the overall gain, but also to shift the peak. This peak shift explains why the low-bias lasing mode is always red-shifted compared to the high-bias lasing mode.

D. Switchable Spacing

The three devices were made from the same wafer, but because of their different structures, the characteristics, including threshold current density and lasing wavelength, of the three lasers were different. Nevertheless, at different pump-current densities, all three devices showed lasing-wavelength bistability. There is also a remarkable characteristic that stands out when the switchable spacings of all three devices (Fig. 8) are plotted together. First, the spacing between modes for device 2 and device 3 at the lowest current overlap almost exactly
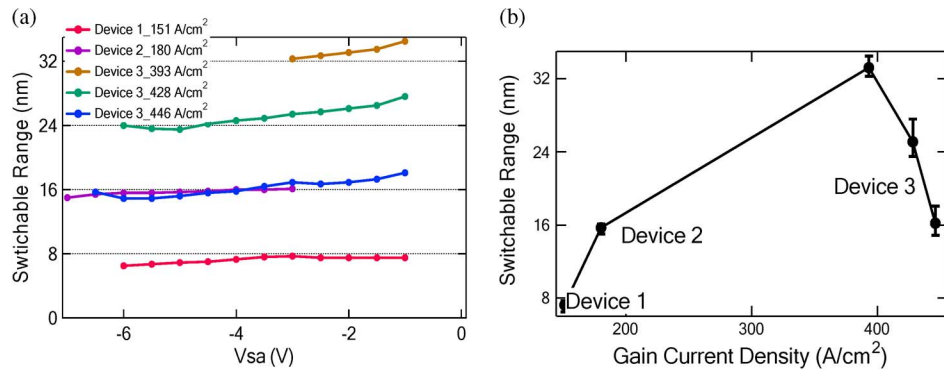
Fig. 8. Comparison of the switchable range of the three devices. (a) Different saturable absorber bias voltage. (b) Different gain-current densities. The error bars are the maximum and minimum ranges.
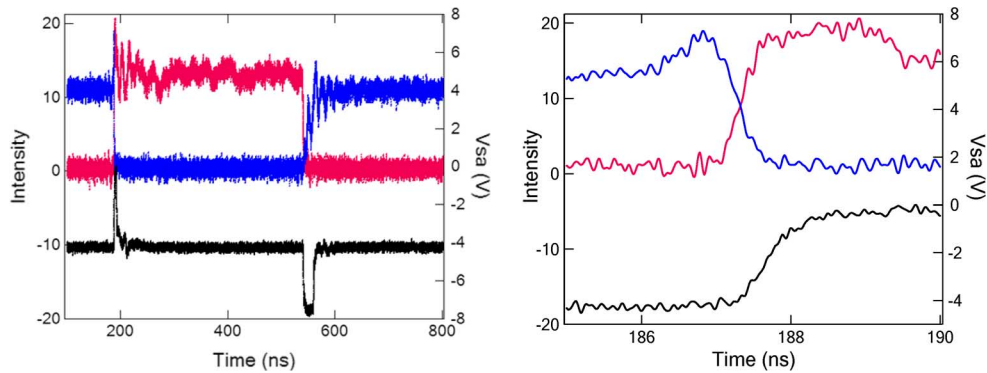
Fig. 9. Switch wavelength between two bistable wavelengths in device three. The red line is the intensity of long wavelength branch (1170 nm), the blue line is the intensity of short wavelength branch (1140 nm), and the black line is the V_{sa} voltage.

throughout the entire bistable range. Second, the switching occurs in discrete steps. Observed values are 7 nm, 16 nm, 25 nm, and 33 nm, all are roughly multiples of 8–9 nm. This behavior is especially interesting, because there are only two modes lasing at one time. The spacing is maintained for widely spaced modes even without the intermediate modes being active.

Time-resolved and spectral hole-burning measurements have shown that the homogeneous linewidth of InGaAs self-assembled QDs is roughly 10 nm at room temperature [16]. The reverse biased section is depleted of carriers, therefore, this width is a reasonable value to assume for the QDs in this section of the laser. To avoid excessive cross-saturation in the absorber region, modes must be spaced by more than the homogeneous linewidth, a criterion for bistable operation, as explained above. With this reasoning we could expect to never observe bistability of two modes that are separated by less than about 10 nm. This fact would also explain the similar spacing seen for different devices, as it is the optical properties of the quantum dots that set the scaling.

More difficult to explain is the consistent spacing of widely separated modes in integer multiples of 8–9 nm. This strongly suggests that although only two modes are seen to lase at one time, the other dormant modes still play a role in the laser dynamics.

E. Switching Time

The wavelength hysteresis loop for a QD diode laser could be used for applications that require switching between wave-lengths on a short time scale. When the saturable absorber is biased in the middle of the hysteresis loop, the output wavelength can be switched by an ultrafast electrical pulse of the required polarity. Since no current is injected into the saturable absorber region, the modification of the saturable absorber that selects the lasing mode should be as fast as the pulse injected. Therefore, the lower limit of switching time between the two stable states for a two-section diode laser is determined by the saturation recovery time of the saturable absorber section, as in [7]. In quantum dots, carrier recovery time can be subpicosecond [14]. In our case, the output of the diode laser is a pulse train, and a minimum of one round-trip is needed for the next lasing state to be established. This time scale is longer than the saturation recovery in our absorber, therefore, the wavelength-switching time should be on the order of the round-trip time of the diode laser.

To measure the switching time we dispersed the output of device three with a grating and measured each wavelength mode independently. A high-speed electrical pulse was applied to the saturable absorber, and output power data was collected with two high-speed photodiodes and an oscilloscope. The measured switching dynamics are presented in Fig. 9. If we define the switching time to be measured is the time from 90% intensity of the wavelength one to 90% intensity of the wavelength two, then the time to switch from the short wavelength branch to long wavelength branch is about 150 ps. In this case the switch occurs faster than the voltage pulse, indicating that the jump in wave-

length takes place on a narrow voltage range. This measured switching time is only about 2 round trips time of the laser.

V. CONCLUSION

In conclusion, wavelength bistability is studied in two-section quantum-dot lasers. Hysteresis and bistability in the lasing wavelengths are observed when the reverse bias voltage is varied on the saturable absorber. The wavelength bistability mechanism is based on the interplay of saturation and the QCSE in the laser. All three devices have bistability, but with different ranges. We have demonstrated the ability to tune this switching range over more than 30 nm with simple changes in the linear gain or absorption present in the devices. The contrast ratio for the two branches is very high. When one wavelength starts lasing, the other is totally quenched. The measured switching time between bistable wavelengths is 150 ps. We believe wavelength bistable devices such as these can be employed as high-speed switches or optical memories in next generation all-optical networks.

REFERENCES

[1] H. Kawaguchi, "Bistable laser diodes and their applications: State of the art," *IEEE J. Sel. Topics Quantum Electron.*, vol. 3, no. 5, p. 1254, 1997.

[2] H. Kawaguchi, T. Mori, Y. Sato, and Y. Yamayoshi, "Optical buffer memory using polarization-bistable vertical-cavity surface-emitting lasers," *Jpn. J. Appl. Phys. Part 2–Lett. & Expr. Lett.*, vol. 45, no. 33–36, p. L894, 2006.

[3] I. White, R. Penty, M. Webster, Y. J. Chai, A. Wonfor, and S. Shahkooh, "Wavelength switching components for future photonic networks," *IEEE Commun. Mag.*, vol. 40, no. 9, p. 74, 2002.

[4] E. Tangdiongga, X. L. Yang, Z. G. Li, Y. Liu, D. Lenstra, G. D. Khoe, and H. J. S. Dorren, "Optical flip-flop: Based on two-coupled mode-locked ring lasers," *IEEE Photon. Technol. Lett.*, vol. 17, no. 1, p. 208, 2005.

[5] X. D. Huang, A. Stintz, H. Li, A. Rice, G. T. Liu, L. F. Lester, J. Cheng, and K. J. Malloy, "Bistable operation of a two-section 1.3-mm InAs quantum dot laser—Absorption saturation and the quantum confined Stark effect," *IEEE J. Quantum Electron.*, vol. 37, no. 3, p. 414, 2001.

[6] O. Qasaimeh, W. D. Zhou, J. Phillips, S. Krishna, P. Bhattacharya, and M. Dutta, "Bistability and self-pulsation in quantum-dot lasers with intracavity quantum-dot saturable absorbers," *Appl. Phys. Lett.*, vol. 74, no. 12, p. 1654, 1999.

[7] H. Uenohara, R. Takahashi, Y. Kawamura, and H. Iwamura, "Static and dynamic response of multiple-quantum-well voltage-controlled bistable laser diodes," *IEEE J. Quantum Electron.*, vol. 32, no. 5, p. 873, 1996.

[8] H. Shoji, Y. Arakawa, and Y. Fujii, "Fast bistable wavelength switching characteristics in 2-electrode distributed feedback laser," *IEEE Photon. Technol. Lett.*, vol. 2, no. 2, p. 109, 1990.

[9] M. Feng, N. A. Brilliant, S. T. Cundiff, R. P. Mirin, and K. L. Silverman, "Wavelength bistability in two-section mode-locked quantum-dot diode lasers," *IEEE Photon. Technol. Lett.*, vol. 19, no. 9–12, p. 804, 2007.

[10] M. A. Cataluna, W. Sibbett, D. A. Livshits, J. Weimert, A. R. Kovsh, and E. U. Rafailov, "Stable mode locking via ground- or excited-state transitions in a two-section quantum-dot laser," *Appl. Phys. Lett.*, vol. 89, no. 8, 2006.

[11] A. E. Siegman, *Lasers*. Sausalito, CA: University Science Books, 1986.

[12] J. D. Murray, *Mathematical Biology I: An Introduction*. New York: Springer-Verlag, 2003.

[13] C. F. Lin and P. C. Ku, "Analysis of stability in two-mode laser systems," *IEEE J. Quantum Electron.*, vol. 32, no. 8, p. 1377, 1996.

[14] P. Borri, W. Langbein, J. M. Hvam, F. Heinrichsdorff, M. H. Mao, and D. Bimberg, "Spectral hole-burning and carrier-heating dynamics in InGaAs quantum-dot amplifiers," *IEEE J. Sel. Topics Quantum Electron.*, vol. 6, no. 3, p. 544, 2000.

[15] P. Borri, W. Langbein, S. Schneider, U. Woggon, R. L. Sellin, D. Ouyang, and D. Bimberg, "Relaxation and dephasing of multiexcitons in semiconductor quantum dots," *Phys. Rev. Lett.*, vol. 89, p. 18, 2002.

[16] P. Borri, W. Langbein, S. Schneider, U. Woggon, R. L. Sellin, D. Ouyang, and D. Bimberg, "Exciton relaxation and dephasing in quantum-dot amplifiers from room to cryogenic temperature," *IEEE J. Sel. Topics Quantum Electron.*, vol. 8, no. 5, p. 984, 2002.

[17] B. Alen, F. Bickel, K. Karrai, R. J. Warburton, and P. M. Petroff, "Stark-shift modulation absorption spectroscopy of single quantum dots," *Appl. Phys. Lett.*, vol. 83, no. 11, p. 2235, 2003.

[18] M. G. Thompson, A. R. Rae, M. Xia, R. Penty, and I. H. White, "InGaAs quantum-dot mode-locked laser diodes," *IEEE J. Sel. Topics Quantum Electron.*, vol. 15, no. 3, p. 661, 2009.

Mingming Feng received the B.S. degree and the M.S. degree in physics from East China Normal University, Shanghai, China, in 1999 and 2002, respectively. He received the Ph.D. degree in physics from the University of Colorado at Boulder in 2009.

He is currently a research associate in the optoelectronics division at the National Institute of Standards and Technology, Boulder, CO. His research interests include fabrication and characterization of semiconductor devices, optical spectroscopy on semiconductor materials, and ultrafast lasers.

Steven T. Cundiff received the B.A. degree in physics from Rutgers University, New Brunswick, NJ, in 1985, and the M.S. and Ph.D. degrees in applied physics from the University of Michigan in 1991 and 1992, respectively.

He spent two years as an Alexander von Humboldt Fellow at the University of Marburg, Germany, and then joined Bell Laboratories, Holmdel, NJ, as a postdoctoral Member of Technical Staff. In 1997 he joined JILA, a joint institute between the University of Colorado and the National Institute of Standards and Technology (NIST), in Boulder, Colorado.

Dr. Cundiff is a Fellow of JILA, a Physicist with the NIST Quantum Physics Division and a Professor Adjoint in the University of Colorado Department of Physics and Electrical and Computer Engineering Department. He is a Fellow of the Optical Society of America and of the American Physical Society.

Richard P. Mirin (M'97–SM'05) received the B.S. degree in electrical engineering from the University of California at Berkeley in 1990 and the M.S. and Ph.D. degrees in electrical engineering in 1992 and 1996, respectively, from the University of California at Santa Barbara.

Upon completion of the Ph.D. degree, he joined the Optoelectronics Division of the National Institute of Standards and Technology (NIST) in Boulder, CO. He is currently the Project Leader for the Nanostructure Fabrication and Metrology Project at NIST. The project's research is focused on precision spectroscopy of semiconductor quantum dots and the applications of quantum dots for single photon sources and detectors. He has published more than 70 papers and 100 conference presentations and proceedings.

Dr. Mirin is a senior member of IEEE and a member of the Optical Society of America.

Kevin L. Silverman received the B.S. degree in physics from Bucknell University in 1996. He received the M.S. and Ph.D. degrees in physics from the University of Colorado at Boulder in 2000 and 2002, respectively.

He is currently a staff member in the optoelectronics division at the National Institute of Standards and Technology in Boulder, CO. His research interests include optical spectroscopy of semiconductor nanostructures and fabrication of quantum dot-based devices.